J Solid State Electrochem (2011) 15:2469–2475
DOI 10.1007/s10008-011-1455-z

ORIGINAL PAPER

Bismuth nanoparticles electrooxidation: theory and experiment

Kh. Z. Brainina · Leonid Gdalievich Galperin · Ludmila Aleksandrovna Piankova · Natalia Yurievna Stozhko · Aidar Marksovich Myrzakaev · Olga Romanovna Timoshenkova

Received: 4 May 2011 / Revised: 11 May 2011 / Accepted: 13 May 2011 / Published online: 11 June 2011

Abstract The article presents the findings of microscopic and electrochemical studies of electrooxidation of bismuth particle of varying sizes. Bismuth particles were immobilized on the surface of indifferent carbon containing screen-printed electrodes. The calculations and experimental studies demonstrated that the transition from macroparticles to nanoparticles caused a shift of the maximum current potential of bismuth oxidation into the area with more negative potentials. A positive correlation between experimental and calculated data confirms once again a relevant application of the earlier proposed mathematical model and the possible use of the shift of the maximum current potential of electrooxidation to describe electrochemical activity and energy properties of metal nanoparticles.

Keywords Bismuth · Nanoparticles · Size effect · Electrochemical oxidation · Electron microscopy

Authors dedicate this paper to the 65th birthday of Prof. George Inzelt and wish him many years of luck and success.

K. Z. Brainina (✉) · L. A. Piankova · N. Y. Stozhko
Ural State University of Economics,
8 Marta St, 62,
Yekaterinburg 620144, Russia
e-mail: baz@usue.ru

L. G. Galperin
Ural Federal University,
Mira St, 19, A-203,
Yekaterinburg 620002, Russia

A. M. Myrzakaev · O. R. Timoshenkova
Institute of Electrophysics, Russian Academy of Science,
Ural Branch,
Amundsena St, 106,
Yekaterinburg 620016, Russia

Introduction

Physical properties of nanosystems differ significantly from macrosystems. These differences include dependence of magnetoresistance, melting temperature, surface tension, and optical, catalytic, and electrochemical properties on the metal particle radius [1–8]. Compton et al. [9–12] have analyzed the effect of geometric factors (particles shapes, particles distribution, and diffusion zones) on the electrochemical behavior of nanoparticles. The role of thermodynamics in nanopartcles electrochemistry was described in [13, 14]. Due to significance of sensors, based on nanoparticles, development [9, 15], and nanoparticles characterization, the approach described in [13, 14] seems to be useful as a source of information for analytical and material chemistry.

The goals of the proposed work are to continue the abovementioned studies; to determine the size and energy effects on the shape of experimental voltammograms, which describe electrooxidation of bismuth nanoparticles; to compare the calculated and experimental data; and to justify the use of voltammograms for characterization of nanostructures.

Experimental section

Materials, instruments and methods

Bismuth (III) nitrate pentahydrate (≥98.0%) and sodium borohydride (99.99%) were supplied by Sigma–Aldrich. Bismuth nanoparticles obtained by gaseous-phase condensation (Bi_g) were kindly provided by the Institute of Physics of Metals, Russian Academy of Science, Ural Branch.

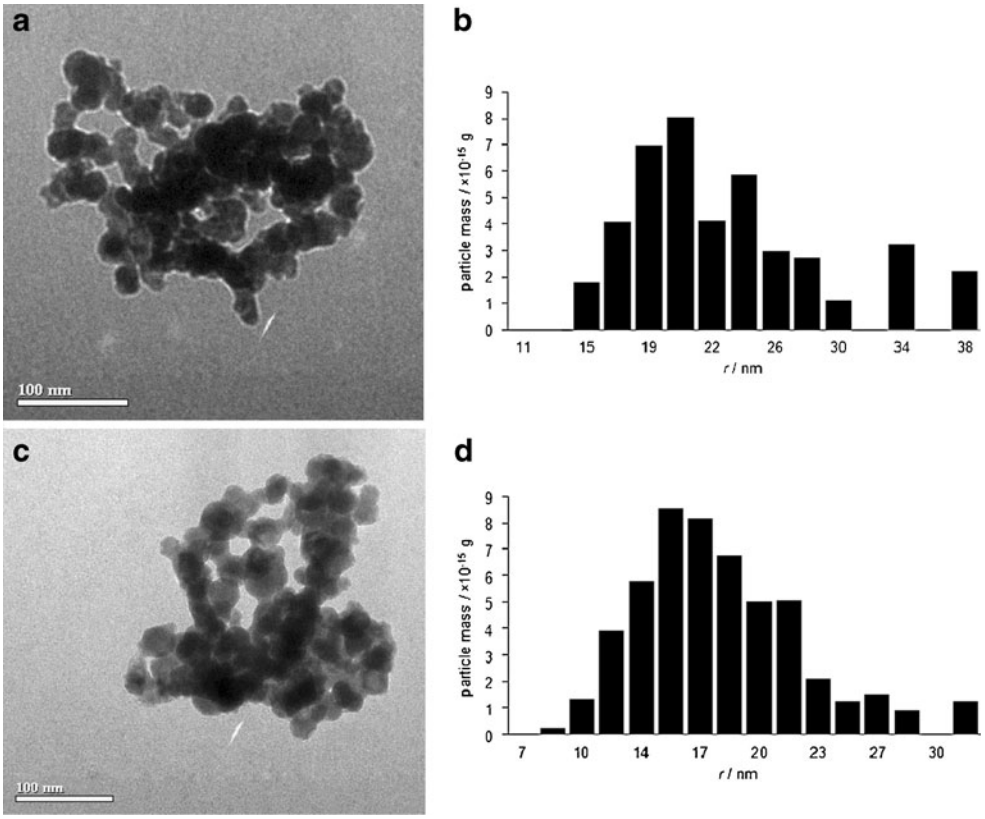

Fig. 1 TEM images of Bi_g (**a**) and Bi_c (**c**) and bar charts of particle distribution (**b**, **d**), respectively

All solutions were prepared using deionized water with a resistivity of no less than 18 MΩ cm, obtained with the membrane system DVS-M/1NA (18)-N (Russia).

Bismuth nanoparticles were synthesized with the use of a magnetic stirrer with heating IKA RCT basic (Germany).

Microscopic studies of bismuth nanoparticles sol were performed with the transmission electron microscope (TEM) JEM-2100 (Japan) with LaB_6 cathode operating at an accelerating voltage of 200 kV (point resolution, 0.19 nm; line resolution, 0.14 nm). Before the microscopic examination, bismuth sols were kept in an ultrasonic field generated by the ultrasonic processor VCX 750 (USA), with the capacity of 300 W for 30–60 s. Then, a drop of suspension was placed onto amorphous carbon film 5 to 6 nm thick and located on a standard copper grid of the TEM. The scanning electron microscope LEO 982 (Germany) and JEM-200CX (Japan) was used to characterize nanoparticles size and distribution on the electrode surface by scanning electron microscopy (SEM).

Electrochemical behavior of bismuth particles was examined by using IVA-5 (Russia), a semiautomatic inverse voltammetric analyzer interfaced to a personal computer and a three-electrode electrochemical cell. A glassy carbon rod was used as an auxiliary electrode, a saturated silver chloride electrode (SCE) (E=0.22 V vs NHE) as a reference electrode. Screen-printed carbon electrodes (SPCE) with carbon-containing ink CIRCALOK 6971 base (Lord, USA) and with the area of 0.10 cm^2 (manufacturer: IVA, Russia) modified with bismuth particles or coated with electrodeposited bismuth film was used as working electrodes.

Anodic voltammograms of bismuth were recorded at a linear potential sweep in the range from −0.2 to 0.5 V at a scan rate 0.1 V s^{-1} using 0.1 M HNO_3 as a background electrolyte. The peak of bismuth oxidation potential (E, volts), the maximum current (I, microampere), and quantity of electricity (Q, microcoulomb) which corresponded to the quantity of substance participating in the electrochemical process, were measured. Q was determined by graphical integration of the area below the anodic voltammograms of bismuth oxidation. All potentials are given relative to SCE.

Synthesis of bismuth nanoparticles

Bismuth (Bi_c) nanoparticles were synthesized by chemical reduction of aqueous solution of Bi $(NO_3)_3$ with sodium borohydride. Freshly prepared $NaBH_4$ was added to a boiling solution containing 1 mM Bi $(NO_3)_3$ with vigorous stirring (1,200 rpm) and boiled for another 10 min. Then, the sol was cooled to room temperature.

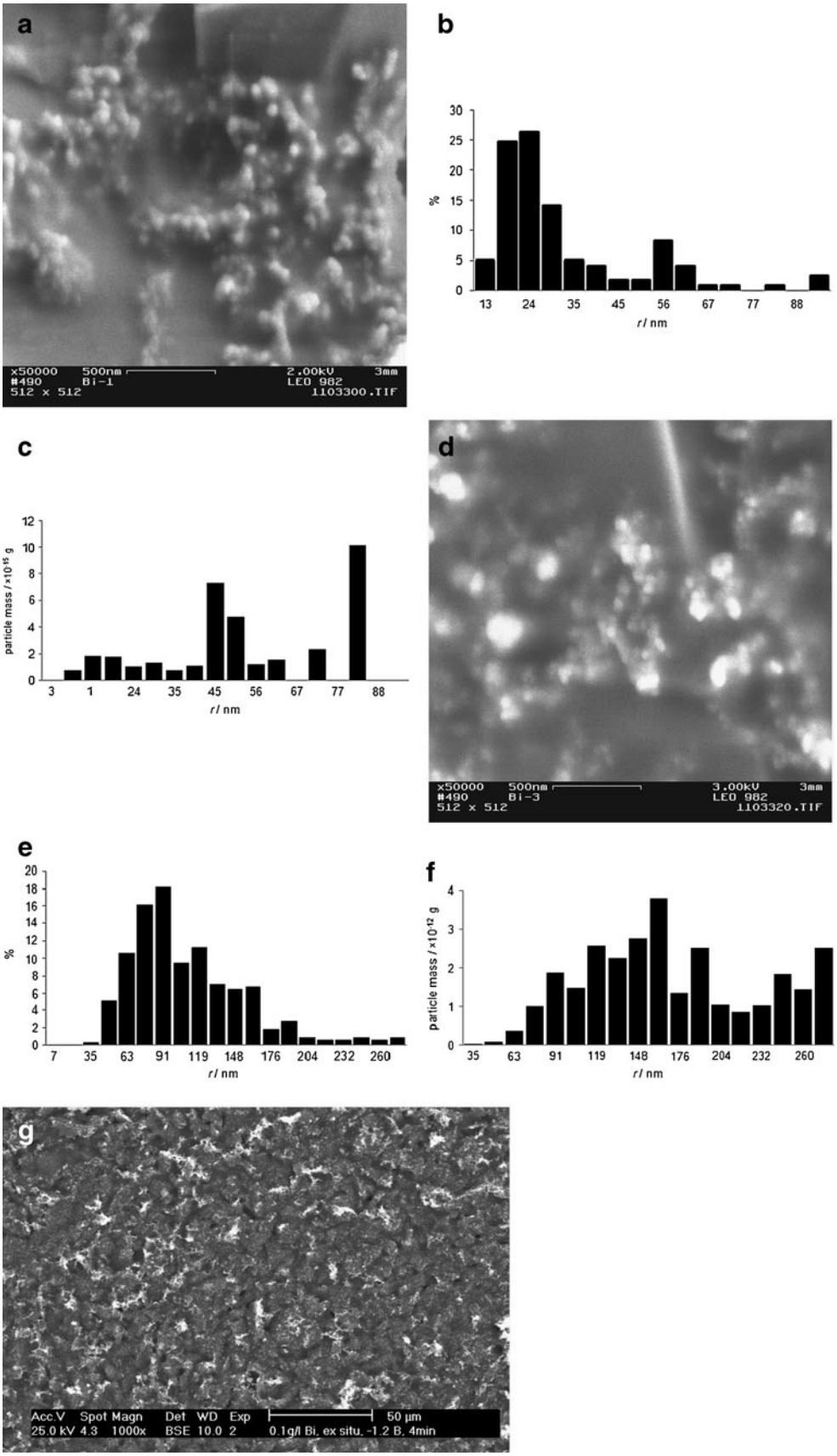

Fig. 2 SEM images of bismuth particles Bi_g (**a**), Bi_c (**d**) (×50,000, LEO 982) and bismuth film electrochemically deposited on SPCE surface Bi_f (**g**) (×1,000, JEM-200CX), and bar charts of particles distribution on SPCE surface by size (**b**, **e**) and mass (**c**, **f**), respectively

Table 1 Parameters for calculating voltammograms of bismuth particles electrooxidation

Parameter	Value
M—bismuth molar (atomic) mass	209 g mol^{-1}
ρ—bismuth density	9.747 g cm^{-3}
σ—surface tension of bismuth on the boundary with air at t 271 °C [16]	382 dyne cm^{-1}
n—number of electrons participating in the rate-determining step of the electrode process [17]	1
δ—fraction of particles of the particular size	Relative units
$E°$—standard (formal) electrode potential of the system Bi^{3+}/Bi [18]	−0.007 V[a]
$\Delta G°$—Gibbs free surface energy	J mol^{-1}
k_s—constant of the electrode process rate	cm s^{-1}
α—electrode process transfer coefficient	0.5

[a] The value is taken from ([18], p.742 and 770, Pourbaix diagram) for pH=1.4. $E°$=0.215 V SHE or −0.007 vs. Ag/AgCl sat

Preparation of the electrodes

Bismuth particles were immobilized on the surface of SPCE. A few microliters of sol were placed on the working area of the electrode and left at room temperature in open air until completely dry. The bismuth film (Bi_f) was plated by electrolysis of a stirring solution containing 4.8×10^{-4} M Bi (III), at a potential −0.8 V for 5 min. Cementit 3,172 glue was applied to isolate the working area of the electrodes.

Results and discussion

Characterization of the bismuth sol

Figure 1 shows TEM images of bismuth particles and bar charts demonstrating the distribution of particles by mass (average mass radius). The average mass radius is 20.5 nm (Bi_g) and 17 nm (Bi_c). Bismuth particles in synthesized sols generally have a shape closer to spherical.

Characterization of bismuth particles on the electrode surface by SME

Figure 2 shows SEM images of the SPCE surfaces, modified with bismuth nanoparticles of different sizes (a, d) and with bismuth film. Bismuth nanoparticles are shown as white spots mainly located on the elevated (gray) areas but virtually absent in the lower zones (black areas). Figure 2 shows that surface morphology of the examined bismuth electrodes varies significantly. Particles on the surface of SPCE/Bi_g are uniformly allocated. The distance between the particles exceeds their size 3–30 times. On the surface of SPSE modified with Bi_c (SPSE/Bi_c) (Fig. 2d) both larger and smaller particles are observed. The average

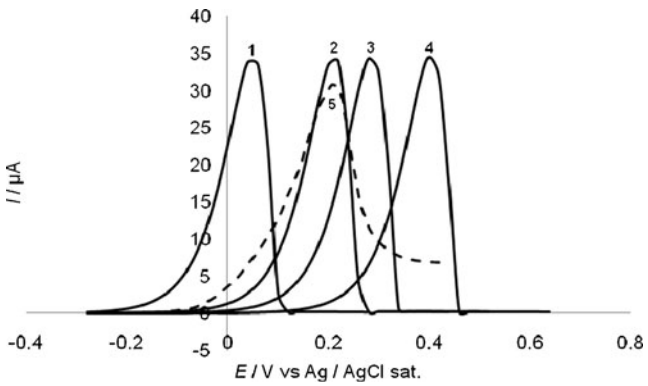

Fig. 3 Calculated (*1–4*) and experimental (*5*) voltammograms for bismuth film electrooxidation. Background: 0.1 M HNO_3, υ= 0.1 V s^{-1}. Calculated parameters: r=1 μm; Q=40 μC; $\Delta G°$= 24.57 J mol^{-1}; δ=1; k_s (cm s^{-1})—10^{-6} (*1*); 4.25×10^{-8} (*2*); 10^{-8} (*3*); 10^{-9} (*4*). Other parameters: as given in Table 1

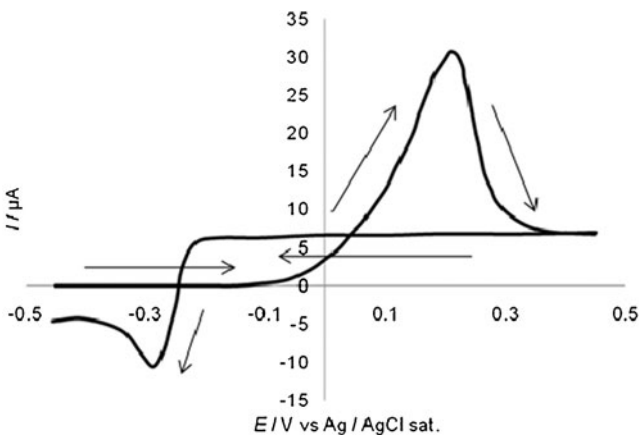

Fig. 4 Cyclic voltammogram of Bi_f. Background: 0.1 M HNO_3, υ= 0.1 Vs^{-1}. The *arrows* show the direction of the forward and reverse scan within the range from −0.47 to 0.47 V

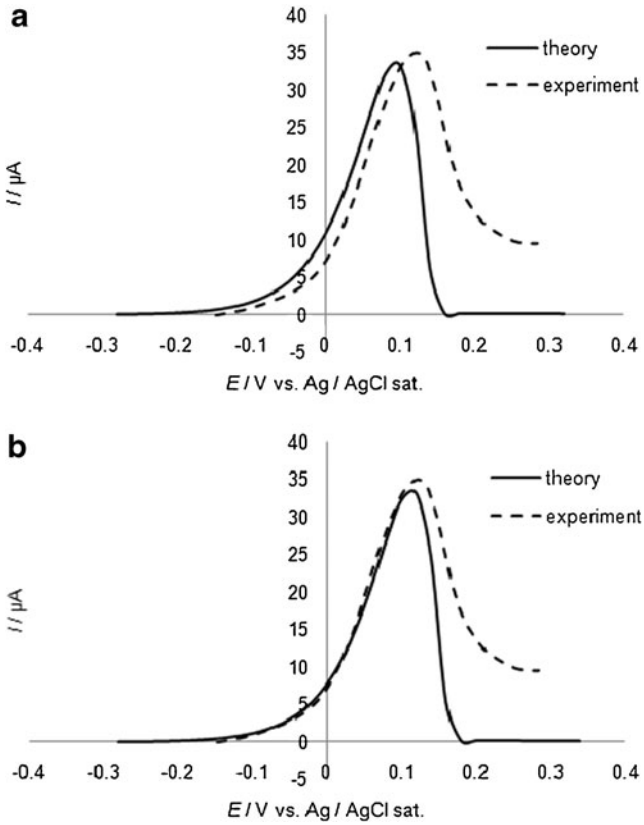

Fig. 5 Calculated and experimental voltammograms for bismuth nanoparticles electrooxidation. Background: 0.1 M HNO_3, υ= 0.1 V s^{-1}. Calculation parameters: r=105 (**a**) and 150 nm (**b**), Q= 40 μC, $\Delta G°$=234.0 (**a**) and 163.8 J mol^{-1} (**b**), δ=1. Other parameters: as given in Table 1

mass size of particles on the surface of the SPCE/Bi_c is 150 nm. As can be seen on Fig. 2g, the surface of SPCE modified with Bi_f is not completely covered with bismuth. The size of the SPCE surface areas covered with Bi_f varies from 2 to 13 μm.

Figure 2 shows the bar charts that characterize distribution of bismuth particles by size (b, e) and by mass (c, f). It can be seen that these values do not coincide. Statistically averaged radius of Bi_g on the surface is 24 nm, while the average mass radius of Bi_g is 56 nm. Statistically averaged radius of Bi_c on the surface is 91 nm, while the average mass radius of Bi_C is 150 nm.

Calculated and experimental data

The data used for calculating are presented in Table 1.

Most of the parameters are reference values or calculated on their basis. Thus, the value of $\Delta G°$ was calculated as:

$$\Delta G^{\circ} = S \times \sigma \quad (1)$$

$$S = 4\pi r^2 N \quad (2)$$

where S is the total surface area of one mole of the particles localized on the electrode surface and N is the number of particles of the size under the investigation in one mole.

The number of electrons participating in the electrode process was taken as 1 in accordance with [17], where the rate determining stage is $Bi \leftrightarrow Bi^{+}$. In order to determine k_s, a set of voltammograms for the film electrode was calculated with various k_s and the most corresponding one to the experimental voltammogram of the bismuth film oxidation was selected.

Figure 3 shows the calculated and experimental voltammograms for bismuth film oxidation. The calculations were based on the mathematical model and program, described in [13], with r=1 μm (the particles of this size have the properties of the bulk metal, such as the film is), Q=40 μC, δ=1, $\Delta G°$=24.57 J mol, υ=0.1 V s^{-1}, $k_s=10^{-6}$ (1); 4.25×10^{-8} (2), 10^{-8} (3), 10^{-9} cm s^{-1} (4). A solution containing 0.1 M HNO_3 was used to record the experimental curve.

The curve calculated for $k_s=4.25\times10^{-8}$ cm s^{-1} is virtually identical to the experimental voltammogram, which clearly indicates the irreversible nature of the process. The latter is also confirmed by the shape of the cyclic voltammogram (Fig. 4), demonstrating significant (0.502 V) difference between potentials of anodic and cathodic peaks.

Considering the data presented in Figs. 3 and 4, $k_s=4.25\times10^{-8}$ cm s^{-1} was taken for further calculations.

Our previous studies [13, 14] demonstrated strong dependence of the peak potentials of voltamperogams (their position on the axis of potentials) on the particle size.

Figure 5 shows the experimental voltammograms and curves, which were calculated using the data (particle radius) taken from the bar charts in Fig. 2e, f. As it is seen, the calculated and experimental data have better agreement in the second case, which is understandable if we take into account the fact that the electrode process is determined by the mass of the participating agents. The data obtained from the calculation of particle size by mass were used for further calculations. The correctness of the choice is confirmed by the data shown in Fig. 6.

Figure 6 shows the experimental and calculated voltammograms of electrooxidation of bismuth particles of different sizes. The experimental and calculated curves practically coincide. Figure 6d allows to compare all the experimental voltammograms (a–c). With decreasing particle size, a shift of the calculated and experimental curves towards negative potentials is clearly observed, which is

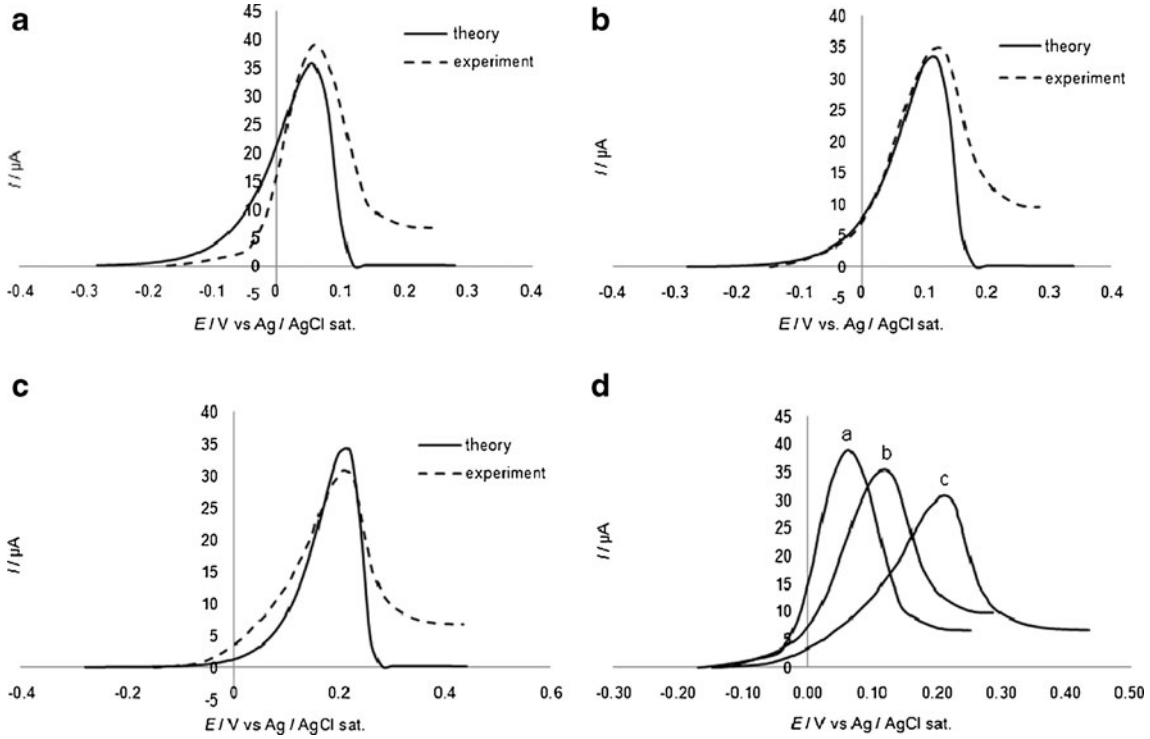

Fig. 6 Calculated and experimental voltammograms for bismuth nanoparticles electrooxidation (**a**, **b**), immobilized on SPCE surface; for bismuth film (**c**) electrochemically deposited on SPCE surface; and experimental voltammograms for electrooxidation of bismuth particles of different sizes (**d**). Supporting electrolyte: 0.1 M HNO_3, υ= 0.1 V s^{-1}. Calculation parameters: r=56 nm, Q=41 μC, δ=1, $\Delta G°$= 463.6 J mol^{-1} (**a**); r=150 nm, Q=38.7 μC, δ=1, $\Delta G°$=163.8 J mol^{-1} (**b**); r=1 μm, Q=40 μC, $\Delta G°$=24.57 J mol^{-1}, δ=1 (**c**). Other parameters: as given in Table 1

consistent with theoretical assumptions [13] and previously obtained experimental data [14].

Conclusion

The validity of the previously proposed mathematical model of electrooxidation of metal nanoparticles which takes into account Gibbs free surface energy [13] is once again [14] confirmed by the agreement between the calculated and experimental data given above. In the previous work [14], this agreement was demonstrated for electrooxidation of gold nanoparticles. This work illustrates the agreement by studying electrooxidation of bismuth nanoparticles. The available data suggest that the shift in the peaks of voltammograms describing electrooxidation of nanoparticles toward negative values is caused by higher magnitude of Gibbs free surface energy along with decrease in particle radius. Since this shift is quantitatively related to the value of Gibbs free surface energy [13], it is possible to formulate the reverse problem: to estimate the magnitude of Gibbs free surface energy on the basis of experimentally recorded difference of peak potential for voltammograms describing electrooxidation of macro/micro- and nanoparticles.

Acknowledgments The authors express their deep gratitude to the financial support of the Government of Sverdlovsk Oblast "Priority directions of development of nanotechnologies for Innovative Development for Sverdlovsk region in 2008–2010 years" and RFFI (Project # 07-03-96070-p_ural_a). The authors also thank A. E. Ermakov for providing bismuth nanoparticles obtained by gaseous-phase condensation.

References

1. Wang J, Cao G, Lia Y (2003) Mater Res Bull 38:1645–1651
2. Jiang Q, Zhang S, Zhao M (2003) Mater Chem Phys 82:225–227
3. Liu X, Atwater M, Wang J, Huo Q (2007) Colloids Surf B 58:3–7
4. Wang YW, Hong BH, Kim KS (2005) J Phys Chem B 109:7067–7072
5. Kalimuthu P, John SA (2008) J Electroanal Chem 617:164–170
6. Inasaki T, Kobayashi S (2009) Electrochim Acta 54:4893–4897

7. Abdullin TI, Bondar OV, Nikitina II, Bulatov ER, Morozov MV, Hilmutdinov AKh, Salakhov MKh, Çulha M (2009) Bioelectrochem 77:37–42
8. Stozhko N, Yu, Malakhova NA, Byzov IV, Brainina KhZ (2009) J Anal Chem 64:1176–1185
9. Ward Jones SE, Chevallier FG, Paddon CA, Compton RG (2007) Anal Chem 79:4110–4119
10. Streeter I, Baron R, Compton RG (2007) J Phys Chem C 111:17008–17014
11. Ward Jones SE, Campbell FW, Baron R, Xiao L, Compton RG (2008) J Phys Chem C 112:17820–17827
12. Ward Jones SE, Zheng SH, Jeffrey CA, Seretis S, Morin S, Compton RG (2008) J Electroanal Chem 616:38–44
13. Brainina KhZ, Galperin LG, Galperin AL (2010) J Solid State Electrochem 14:981–988
14. Brainina KhZ, Galperin LG, Vikulova EV, Stozhko NYu, Murzakaev AM, Timoshenkova OR, Kotov YuA (2011) J Solid State Electrochem 15:1049
15. Malakhova NA, Stojko NY, Brainina KhZ (2007) Electrochem Commun 9:221–227
16. Yuan Z, Fan J, Li J, Ke J, Kusuhiro M (2004) Scand J Metall 33:338–346
17. Wilson PT (1972) The kinetics of the anodic dissolution of bismuth in acid solutions: PhD. Auckland
18. Nikolskiĭ NP (ed) (1965) Spravochnik khimika, vol 3. Khimiâ, Moskva, p 742